Published in final edited form as:
J Med Chem. 2012 December 13; 55(23): 10674–10684. doi:10.1021/jm301345v.

Structure Dependence of Long-Chain [^{18}F]Fluorothia Fatty Acids as Myocardial Fatty Acid Oxidation Probes

Mukesh K. Pandey[1,2], **Anthony P. Belanger**[2], **Shuyan Wang**[2], and **Timothy R. DeGrado**[1,2,*]

[1]Department of Radiology, Mayo Clinic, Rochester MN

[2]Department of Radiology, Brigham and Women's Hospital, Harvard Medical School, Boston, MA

Abstract

In-vivo imaging of regional fatty acid oxidation (FAO) rates would have considerable potential for evaluation of mammalian diseases. We have synthe sized and evaluated ^{18}F-labeled thia fatty acid analogues as metabolically trapped FAO probes to understand the effect of chain length, degree of unsaturation and placement of the thia-substituent on myocardial uptake and retention. 18-[^{18}F]fluoro-4-thia-(9*Z*)-octadec-9-enoic acid (**3**) showed excellent heart:background radioactivity concentration ratios along with highest retention in heart and liver. Pretreatment of rats with the CPT-1 inhibitor, POCA, caused >80% reduction in myocardial uptake of 16-[^{18}F]fluoro-4-thia-hexadecanoic acid (**2**), and **3** indicating high specificity for FAO. In contrast, 18-[^{18}F]fluoro-4-thia-octadecanoic acid (**4**), showed dramatically reduced myocardial uptake and blunted response to POCA. 18-[^{18}F]fluoro-6-thia-octadecanoic acid (**5**), showed moderate myocardial uptake and no sensitivity of myocardial uptake to POCA. The results demonstrate relationships between structures of ^{18}F-labelled thia fatty acid and uptake, and their utility as FAO probes in various tissues.

Keywords

Fatty acid oxidation; PET; myocardial metabolism

Introduction

Fatty acid oxidation (FAO) plays a pivotal role in energy production in many tissues and is a candidate biomarker for various disease states in cardiology, endocrinology, neurology and oncology. Myocardial FAO is a highly regulated process, governed by fatty acid supply, competing energy substrates, energy demand, oxygen supply, and hormonal status among other factors[1]. The potential diagnostic utility of a noninvasive PET (positron emission tomography) approach to estimate regional FAO rates in the heart becomes apparent as cardiac dysfunction often displays metabolic changes that alter FAO[1] and could be applicable for evaluation of myocardial ischemia or heart failure. According to the metabolic trapping approach for radiotracer design, the ideal radiotracer for myocardial FAO imaging will mimic natural long chain fatty acids in their transport from the bloodstream into myocytes as well as their intracellular trafficking to the mitochondrion for oxidation[1]. FAO

Corresponding Author: Phone: (507) 538-4319. Fax (507) 266-4461. degrado.timothy@mayo.edu.
Present address
Department of Radiology, Mayo Clinic, 200 First Street SW, Rochester MN 55905 USA

Supporting Information
^{1}H-NMR spectra of nonradioactive standards and radio-HPLC chromatograms of compounds used in the present study are available free of charge via the Internet at http://pubs.acs.org.

occurs in the mitochondrion matrix through the cyclical oxidative process of β-oxidation. The overall rate of β-oxidation is dependent on the flux control exerted by a multitude of processes, including fatty acid transport across the cell membrane (CD36/FATP), activation by fatty acyl CoA synthetase, transport into the mitochondrial matrix facilitated by carnitine palmitoyltransferases I and II (CPT-I, CTP-II), carnitine acyl-carnitine translocase (CAT), and the four enzymes responsible for β-oxidation[1]. CPT-I present at the outer mitochondrial membrane often represents the major step for flux control for FAO of fatty acids[1]. Therefore, CPT-I inhibitors such as POCA (sodium 2-[5-(4-chlorophenyl)-pentyl]-oxirane-2-carboxylate) have been extensively employed to reduce FAO rates in experimental studies[2].

The ideal FAO probe that is based on the metabolic trapping concept should follow the flux of fatty acids through at least the initial step(s) of β-oxidation at which point the tracer becomes metabolically trapped. The probe should not undergo esterification into various complex lipids as it renders the accumulation of radioactivity less specific to FAO[1,3–5]. Over the decades, our research has been focused on the potential of radiolabeled thia-substituted long-chain fatty acid analogs as such metabolically trapped probes of FAO in heart and other tissues[2–3,6–9]. The first molecule developed was [^{18}F]FTHA (**1**)[2] (Figure-1) a 6-thia analog, which showed excellent myocardial imaging characteristics. Surprisingly, **1** was found to be metabolized in heart to protein-bound species, presumably metabolic byproducts from β-oxidation. However, **1** lacked specificity in to measure FAO in hypoxic conditions due to maintained myocardial retention of radiotracer[3,8]. Furthermore, metabolite analyses in liver and skeletal muscle tissues revealed a predominant accumulation of **1** in lipid pools, further limiting its application as a general mitochondrial FAO probe[2]. The second tracer developed was a 4-thia analog of palmitic acid, **2** (Figure-1). The 4-thia analog showed enhanced specificity to myocardial FAO, correlating with FAO rates of natural fatty acids in hypoxic conditions[6,7]. However, uptake of **2** in liver was not sensitive to CPT-I inhibition, and there was poor retention of the “metabolically trapped” radioactivity in rat myocardium over a 2 h period[3]. Subsequently, a 4-thia substituted oleic acid analog was developed as **3**[10] (Figure-1). Compound **3** showed enhanced uptake and retention in rat myocardium relative to both **1** and **2**[10]. Pharmacologic inhibition of CPT-1 with etomoxir evoked >80 % decrease in myocardial uptake, demonstrating excellent sensitivity to change in myocardial FAO[10]. The differences in the biodistribution properties of compounds **1–3** raised the questions: what aspects of the structure of **3** were responsible for its favorable myocardial uptake properties and could they be further enhanced? To begin to answer these questions, two additional molecules were designed and evaluated as stearic acid analogs: 18-[^{18}F]fluoro-4-thia-octadecanoic acid (18:0) (**4**) and 18-[^{18}F]fluoro-6-thia-octadecanoic acid (18:0) (**5**) (Figure 1). The in vivo characteristics of **4** and **5** were examined in comparison with those of the previously developed **2** and **3** since these two radiotracers fill the structural gap between the **2** and **3** to investigate the effects of chain length (**2** versus **4**), thia position (**4** versus **5**), and saturation (**3** versus **4**). Our present study provides considerable information on the structural dependence of thia-substituted fatty acid radiotracer uptake and retention in myocardium and provides a stronger basis for rational design of PET imaging probes for FAO.

Results

Synthesis of 18-[^{18}F]fluoro-4-thia-octadecanoic acid (4) and 18-[^{18}F]fluoro-6-thia-octadecanoic acid (5)

Schemes 1 and 2 describe the synthesis of **4** and **5**, respectively. To synthesize the labeling precursor for **4**, 1,14-tetradecadioic acid was converted to 1,14-tetradecane diol (**6**) in two steps: esterification using absolute methanol and catalytic amount of sulfuric acid followed

by LAH (lithium aluminum hydride) reduction in THF(tetrahydrofuran)[11]. The obtained diol was refluxed with 48% aq. HBr to yield 1,14-dibromo-tetradecane (**7**), which on subsequent reaction with methyl 3-mercaptopropanoate in presence of sodium hydride in THF yielded methyl 18-bromo-4-thia-octadecanoate (**8**) as precursor for radiofluorination. The formation of compound **8** was characterized by presence of two triplets peaks in the ^{1}H NMR spectrum, one at δ 3.41ppm for two protons (CH_2Br) and another at δ 2.60 ppm for two protons (CH_2-S). The product formation was further confirmed by carbon NMR, gradient HSQC and HR(EI) mass spectroscopy. The bromo-ester **8** was treated with tetrabutylammonium fluoride in acetonitrile followed by ester hydrolysis to obtain nonradioactive standard (**9**) as a HPLC standard. The formation of **9** was characterized by the appearance of doublet of a triplet (dt) at δ 4.46 ppm for two protons due to the formation of the new carbon fluorine bond (CH_2F) and absence of a triplet peak at δ 3.41 ppm for two protons (CH_2Br). The formation of cold standard **9** was also confirmed and supported by a doublet peak at δ 83.7 – 84.8 ppm due to fluorine-carbon coupling in its carbon NMR. HRMS confirmed the product formation with a molecular ion peak at 320.21755 amu. The radiofluorination of the bromo-ester **8** using cyclotron-produced $K^{18}F$ was carried out under microwave heating (75 °C) as previously described[12]. Radiofluorination proceeded efficiently, with >90% incorporation of [^{18}F]fluoride into the corresponding ester. The [^{18}F]fluoro-ester was quantitatively hydrolyzed by addition of 0.2 N KOH and microwave heating (75 °C) for 2 min. Overall radiochemical yields after semi-preparative HPLC isolation (Rt = 9.4 min) were 30–33% decay-corrected. Radiochemical purity of the product **4** was >99% by radio-HPLC. The product was formulated in 0.5–1.0% BSA (bovine serum albumin) in saline solution and passed through a sterile filter before administration to rats.

The synthesis of the labeling precursor for **5** required a modified approach due to the unavailability of methyl 6-mercaptopentanoate. The methyl 6-mercaptopentanoate (**10**) was obtained on reaction between methyl 5-bromo-pentanoate and thiourea followed by treatment with ethanolic NaOH and subsequent esterification with absolute methanol[13]. Compound **10** was treated with 1,12-dibromo-dodecane (**11**) in the presence of sodium hydride in THF, forming methyl 18-bromo-6-thia-octadecanoate (**12**) as precursor for radiofluorination. Compound **12** was characterized by the proton NMR presence of a triplet at δ 3.42 ppm for two protons (CH_2Br) and another multiplet at δ 2.52- 2.50 ppm for four protons due to the formation of a thioether (CH_2-S-CH_2). The product formation was further supported by carbon NMR and HR(EI) mass spectroscopy. The bromo-ester **12** was also treated with tetrabutylammonium fluoride in acetonitrile followed by ester hydrolysis to obtain nonradioactive standard **13** as nonradioactive HPLC standard. Compound **13** was confirmed by proton and carbon NMR, and HRMS. The radiofluorination, hydrolysis and formulation were carried out in a similar manner as with **4**. The radiochemical yield of the labeled product **5** after semi-preparative HPLC isolation (Rt = 8.7 min) was 30–33% decay-corrected. Radiochemical purity of the product (**5**) by r-HPLC was >99%.

Biodistribution Studies in Rats

Tables 1–4 show the biodistribution data for ^{18}F-radioactivity in rats after intravenous administration of **2–5** at 30 and 120 min post-injection (p.i.). To indicate the sensitivity of the biodisposition of the fatty acid analogs to FAO impairment, data were obtained with and without pretreatment of rats with the CPT-1 inhibitor POCA (sodium 2-[5-(4-chlorophenyl)-pentyl]-oxirane-2-carboxylate)[2,14].

The palmitate analog **2** showed high myocardial uptake at 30 min (0.589±0.257 % ID kg/g, Table 1). However, there was >80% washout of radioactivity from control hearts from 30 to 120 min. The pretreatment of rats with POCA markedly decreased (>90 %) myocardial uptake at 30 min, indicating very high sensitivity of **2** towards FAO. The effect of POCA

was not observed at 120 min due to clearance of **2** from control hearts. The metabolic fate of **2** studied by folch type extraction of heart tissues (Table 5) showed 58.8±19.2 % of activity bound to the protein pellet at 30 min control as compared to 32.8±6.1 % of activity with POCA treated rats at 30 min. Radioactivity in the protein pellet was interpreted as the fraction of radiotracer that had undergone β-oxidation[2,3,5,10]. Inhibition of β-oxidation by POCA results in reduced radioactivity bound to protein and increased radioactivity in organic soluble metabolites (nonmetabolized fatty acid or complex lipids) or to a lesser extent aqueous metabolites [5]. Therefore, these data further supported the sensitivity of **2** to FAO. This effect was more pronounced at 120 min, showing 76.9±10.8 % of radioactivity bound to protein pellet in control hearts as compared to 24.5±5.4 % in POCA hearts (Table 5).

Table 2 summarizes the biodistribution data for **4** (18:0). It showed 1.7 fold higher ($p < 0.05$) heart uptake of tracer at 30 min control rats than 30 min POCA treated rats indicating considerable sensitivity of **4** towards FAO. More importantly, **4** showed longer retention in heart over time as indicated by 120 min control uptake studies. The folch type extraction of heart tissues treated with **4** showed 78.7±3.5 % radioactivity bound with protein pellet at 30 min control supporting sensitivity of the tracer towards FAO. On comparison with **2**, **4** had 1.8 fold lower myocardial uptake at 30 min control but longer retention in the heart. The longer retention was also supported by metabolic studies where it showed 71.5±5.5 % of radioactivity bound to protein pellet at 120 min control.

Table 3 summarizes the biodistribution data for **5** where the sulfur atom replaced the sixth carbon in the stearate analog. CPT-I inhibition by POCA had no effect on myocardial uptake at either time points, indicating poor sensitivity to indicate mitochondrial FAO. Myocardial washout was slow over the 30–120 min period. The retained radioactivity was primarily in the form of protein-bound metabolites in control hearts but in the organic phase of Folch extractions in POCA hearts (Table 5). Similar results were also obtained at the 120 min time point. On comparison to **4**, **5** had similar uptake and retention in heart tissue at 30 min and 120 min controls but uptake of **5** by the heart was found to be less sensitive to POCA treatment.

Table 4 provides the biodistribution data for the oleate analog **3**. Compound **3** showed the highest heart uptake of the four tracers. Myocardial uptake of **3** in control animals was statistically unchanged from 30 to 120 min, demonstrating effective trapping in heart tissue. On treatment with POCA, the heart uptake dramatically decreased at both 30 min (−84%) and 120 min (−90%) time points, indicating very high specificity and sensitivity of **3** for FAO (Figure 2). The folch-type extraction of heart tissues after administration of **3** demonstrated the highest levels of protein binding for all tracers studied (>88%), suggesting highest metabolic conversion to protein-bound metabolites. In control animals, myocardial uptake of **3** was 1.2, 2.2, and 1.6 fold higher ($p < 0.05$) than that of **2**, **4** and **5** at 30 min p.i. (Figure 2) At the 120 min time point, the heart uptake of **3** was 2.6–8.0 fold higher ($p < 0.05$) than the other tracers (Figure 2).

With regard to the whole-body distribution of the tracers, **2** and **4** showed high uptake in liver, followed by heart, bone, kidney and other organs at 30 min in fasted control rats. Compounds **3** and **5** showed highest uptake in liver, followed by heart, kidney, bone and other organs at 30 min control fasted rats. Furthermore, all four tracers (**2–5**) showed highest uptake in liver at 120 min. However, this trend differed slightly in the case of **5** and **3**, where heart showed second highest uptake after liver indicating longer myocardial retention. Hepatic clearance was greater for **2**, **4** and **5** in comparison with **3** (Figure 3) between 30 min and 120 min in control animals. Bone uptake for the all the four tracers was comparable at 120 min, suggesting their equivalent defluorination rates in rat.

Heart:organ ratios for **2–5** at 120 min post-administration of tracers are shown in Figure 4. Heart:blood ratio for **3** was found to be 4.0 fold higher than **2**; 1.8 fold higher than **4** and 3.0 fold higher than **5** ($p = < 0.005$). The heart:muscle ratio for **3** was 3.0, 3.5, and 4.2 fold higher than **2**, **4**, and **5**, respectively ($p = < 0.005$). Furthermore, heart:liver ratios for **3** were 3.3 and 2.5 fold higher than **2** and **5**, respectively ($p = < 0.005$).

Folch-type extraction analysis of tissues showed that **3** is metabolized predominantly to protein-bound species in control hearts (Figure 5). At 120 min, the radioactivity of protein-bound fraction in heart was significantly higher for **3** (89%) relative to **2** (77%), **4** (71%) and **5** (67%) ($p<0.05$). At 30 min, protein-bound, aqueous, and organic fractions in liver and skeletal muscle were similar for **2**, **4** and **5** (Figure 5). However, **3** showed up to 71% ($p<0.01$) and 59% protein-bound fractions in liver and skeletal muscle, respectively (Table 5). The protein-bound fractions of **2**, **4**, and **5** were lower than those for **3** in liver and skeletal muscle, indicating lower FAO-dependent metabolic trapping relative to **3** in these organs.

It was also observed that POCA-treated rats had relatively higher uptake in blood, brain and muscle. For example, POCA-treated rats with **2** and **5** showed 2.7 fold ($p<0.005$) and 2.2 fold ($p<0.005$) higher muscle uptake at 120 min than control rats, respectively. In contrast, such enhancement with POCA-treatment was not observed for **3** and **4**. POCA-treated rats showed ~ 3.0 fold higher fatty acid concentration and reduced glucose concentration in plasma with respect to control rats (Table-6), whereas, triglyceride and lactate concentrations were independent of CPT-I inhibition. As a CPT-I inhibitor, POCA was developed to be a potential anti-diabetic drug. It increases plasma fatty acid levels by lowering the rate of fatty acid clearance from the blood due to decreased β-oxidation in liver, heart and skeletal muscle. Conversely, POCA lowers blood glucose. The decrease in FAO stimulates glucose oxidation in liver, heart, and skeletal muscle to maintain energy status. The higher glucose metabolic rates in these tissues results in a decrease in plasma glucose levels.

MicroPET Studies in Rats

A preliminary microPET imaging study was performed with **2–5** in fasted rats (Figure 6). Initial dynamic images showed rapid blood clearance of all four tracers to low radioactivity concentrations within 2 min p.i. (post injection). Similarly, lung clearance was also very rapid and gave low background to the heart by 2 min p.i. The hepatic uptake of all the four thia fatty acid tracers (**2–5**) was extremely high at 5 min p.i., followed by slow clearance over time. Myocardial uptakes of all four PET probes plateaued at about 10 min but faster clearance was observed with **2**. Whereas, myocardial clearance was nominal for **4**, and **5** but remained stable for **3**. Whole-body images acquired 55–115 min p.i. demonstrated superior myocardial imaging abilities of **3** among the thia fatty acid tracers (Figure 6). The biodistribution data for all four tracers (Tables 1–4) were consistent with MicroPET images (Figure 6). Bone uptake in ribs were seen with all four radiotracers, indicating *in vivo* defluorination in the rat.

Discussion

Fatty acid oxidation (FAO) is the key energy producer in heart, liver and skeletal muscle. Furthermore, it has recently been investigated that the brown adipose tissue plays a vital role in thermogenesis during cold exposure via oxidative metabolism of fat in human adults[15]. A FAO-specific PET imaging technique has a considerable potential to improve existing medical care by determining disease state and progression, and also for evaluation of potential drug therapies targeted to alter FAO rates[16–18]. Several non-thia fatty acid analogs

of palmitic acid labeled with ^{18}F and ^{11}C were studied and documented in literature[4, 19–23]. However, the fate of the radiolabel involves multiple catabolic and anabolic processes and requires complex kinetic models to derive an estimate for FAO[4,19,20–24]. All the radiotracers in the current study were radiolabeled with ^{18}F at the terminal (ω) position, a site known to undergo metabolic defluorination in liver[25]. Although we have previously shown that the label can be stabilized against defluorination if placed at the (ω-3) position[25], the synthesis burden is greatly increased to produce the labeling precursors. Furthermore, subsequent to our early work with (ω-3) labeled tracers, we found that ω-labeling provided satisfactorily stability against defluorination in pigs and humans[3]. Defluorination of ω-labeled F-18 fatty acids in rodents is significant but does not render the present biodistribution data useless since bone uptake is quantitatively a minor contribution of the overall biodistribution.

The present study extends our work on the structure uptake relationship of thia-substituted fatty acid analogs as metabolically trapped probes for PET imaging of FAO[2,3,10]. Thia-substituted FA analogs are designed to undergo metabolic trapping in myocardium after commitment of the FA toward mitochondrial FAO[5]. β-Oxidation of ω-[^{18}F]fluoro, 4- or 6-thia-fatty acid analogs give rise to protein-bound metabolites in the myocardium, putatively explained by β-oxidation dependent decomposition of the thia fatty acid analogs to ω-[^{18}F]fluoro long-chain thiols that covalently react with mitochondrial proteins[2,3]. The sulfur heteroatom mimics the methylene group of normal fatty acids, although subtly increases the local polarity. The sulfur atom was initially inserted at the sixth position in the first thia-fatty acid radiotracer **1**, showing sensitivity towards CPT-I inhibition in the myocardium in a mouse model[2]. However, further studies indicated FAO-independent mechanisms for retention of radiotracer in hypoxic myocardium[2]. Later, other positions of thia-substitutions were investigated and it was found that sulfur substitution at the fourth position of the palmitate analog **2** gave the best correlation with FAO rates in isolated rat hearts in both normoxic and hypoxic conditions[3]. Although **2** showed higher specificity for FAO, it showed suboptimal retention in rat myocardium.

Therefore, we further explored the structure of the natural FAO substrate oleic acid to form the 4-thia oleate analog **3**[10]. The mono-unsaturated **3** (18:1) showed high myocardial uptake and longer myocardial retention measured at 120 min in rat[10] (Table 4 and 5). To increase our understanding of the different biochemical behavior of **2** and **3**, two additional radiotracers **4**, and **5** were synthesized and allowed the study of the effects of chain length (**2** (16:0) versus **4** (18:0)), mono-unsaturation (**4** (18:0) versus **3** (18:1)) and position of thia-substituent (4-thia **4** versus 6-thia **5**). It was observed that **2** (16:0), **4** (18:0) and **5** (18:0) have almost similar myocardial uptake at 30 min. However, the stearate analogs (18:0) showed better retention in the myocardium than **2** at 120 min. Similar to the stearate (18:0) analogs, the mono-unsaturated (18:1) **3** also showed excellent myocardial retention. On comparing the myocardial kinetics of the unsaturated oleate analog **3** to the saturated stearate analog **4**, the presence of mono-unsaturation resulted in more than double myocardial uptake at 30 min with excellent retention of both radiotracers at 120 min. Furthermore, **3** showed the highest protein-bound fractions of ^{18}F-radioactivity in heart homogenates and markedly higher sensitivity to POCA induced inhibition of myocardial uptake and formation of protein-bound metabolites in the heart. Thus, our findings suggest that mono-unsaturation enhances FAO-dependent transport and intracellular trafficking of **3** to the mitochondrion for oxidative metabolic trapping. The inhibition of myocardial uptake and formation of protein-bound metabolites of FTO (and a lesser extent the other FA analogs) with CPT-I inhibition (POCA effect) is a strong indication of mitochondrial trafficking. The significance of this fact is that FTO may serve as a noninvasive biomarker of the flux of fatty acids to the mitochondrion for β-oxidation. We had confirmed in an earlier work with FTP that the tracer had localized to the mitochondrial fraction by ultracentrifugation[3]. Extending the chain length of the palmitate analog (**2)** by two carbons

to form **4** results in similar uptake and metabolic trapping properties but lengthened myocardial retention, suggesting longer retention of the putative radiolabeled long-chain thiol metabolite for **4**.

Thia-substition at the fourth carbon appears to optimize specificity of metabolic trapping to FAO. FAO-dependent metabolism of the 4-thia analogs to protein-bound metabolites in heart was strongly indicated from the finding that pretreatment of rats with the CPT-I inhibitor POCA resulted in dramatic reductions of protein-bound fractions from 70–89% to 20–25%. To further clarify the nature of the protein binding binding of metabolites, a gel electrophoresis experiment was performed with heart and liver homogenates using **2** and **3**. ^{18}F-radioactivity was found to be distributed among at least five different molecular weight proteins across the gels and not specific to one particular protein (data not shown). This finding is consistent with previously reported mechanism of metabolism of thia fatty acids to long-chain thiol fragments which continues to bear the ^{18}F-radiolabel and nonspecifically bind to mitochondrial protein by formation of disulfide bonds through various cysteine residues[5]. Interestingly, the 6-thia fatty acid analog **5** showed no significant change in myocardial uptake in response to CPT-1 inhibition (Table 3) although protein-bound fractions of ^{18}F-radioactivity in heart homogenates were decreased in a manner similar with the 4-thia fatty acid analogs. It appears that **5** was taken up by POCA treated hearts by an amount near to control levels despite the inhibition of FAO at the CPT-1 step. This behavior differs from that previously seen for **1** in POCA-treated mouse hearts where myocardial uptake was reduced by 87 % ($p<5\times10^{-4}$) at 60 min[2]. It is not clear whether this discrepancy is caused by the difference in fatty acid length (C-18 versus C-17), placement of the ^{18}F (ω versus ω-3), or species differences (rat versus mouse). Profound differences in metabolism have been observed for fatty acids differing by as little as one or two methylene groups[2,3,5,10].

Conclusions

Several long-chain, thia-substituted fatty acid analogs were synthesized and preliminarily evaluated in rats as PET probes for myocardial fatty acid oxidation (FAO). The radiosynthesis of **4** and **5** were developed in analogy to those previously developed for **2** and **3**. Biodistribution and PET imaging studies of the tracers were performed to establish a plausible structure-uptake relationship. The enhanced myocardial uptake and metabolic trapping of **3** is primarily due to the presence of mono-unsaturation, whereas improved retention in myocardium can be attributed to the longer chain length. Myocardial uptake and metabolism of 4-thia stearate analogs appears to be more specific to mitochondrial CPT-1 mediated trafficking to the mitochondrion than the 6-thia analog, **5**. Preliminary images of the accumulation of compound **3** in the rat myocardium were clearly superior to those of **2**, **4** and **5**. In summary, **3** remains the most specific and sensitive FAO probe of the 4-thia fatty acid analogs evaluated and warrants further preclinical evaluation.

EXPERIMENTAL SECTION

Materials and Methods

All chemicals and solvents were purchased from Sigma-Aldrich and used as received. Anhydrous solvents were also purchased from Sigma-Aldrich in “sure seal” bottles. TLC analysis of reaction mixtures and products was performed on Merck silica gel 60 F254 TLC plates. Liquid chromatography was carried out on Merck 60 silica gel (32–63 μm). ^{1}H and ^{13}C NMR were recorded on a Varian 600 MHz spectrometer and referenced to $CDCl_3$ (^{1}H NMR:$CDCl_3$ at 7.26 ppm and ^{13}C NMR:$CDCl_3$ at 77.0 ppm). Mass spectral data were obtained from the Mass Spectral Lab of School of Chemical Sciences, University of Illinois, Urbana, Illinois. Analytical HPLC was performed on a Phenomenex Luna C-18 column (5

μm, 4.6 × 250 mm) with a flow rate of 0.8 mL/min. Semi-preparative HPLC was performed on the final ^{18}F labeled product using a Phenomenex Luna C-18 column (5 μm, 10 × 250 mm) with a flow rate of 5.0 mL/min. POCA (sodium 2-[5-(4-chlorophenyl)-pentyl]-oxirane-2-carboxylate) was obtained as a generous gift from Dr. S. John Gatley, Department of Pharmaceutical Sciences, Northeastern University Boston MA. The "5P30 DK 36836" specialized assay core facility of Joslin DERC Boston, MA was used to estimate the plasma concentration of metabolic substrates like glucose, triglyceride, free fatty acid and lactate. All these substrate were measured by standard enzymatic laboratory assay.

Synthesis of methyl 18-bromo-4-thia-octadecanoate (8)—Synthesis of methyl 18-bromo-4-thia-octadecanoate (**8**) was achieved by coupling methyl 3-mercaptopropionate with 1, 14-dibromo tetradecane (**7**) using sodium hydride. To a stirred solution of methyl 3-mercaptopropanoate (500 mg, 4.16 mmol) in dry THF (100 mL) under nitrogen at 0 °C, NaH (100 mg, 4.16 mmol) was added. The resulting solution was stirred for 15 min at 0 °C. A solution of **7** (1.32 g, 3.70 mmol) in THF (10 mL) was then gradually added and the resulting mixture was maintained at 0 °C for 30 min. The mixture was stirred for 3 h at room temperature and quenched with water. After extraction with the dichloromethane, organic layer was dried over Na_2SO_4 and solvent was evaporated under vacuum. The residue was subjected to column chromatography (5:95 ethyl acetate:hexane) to yield **8** (1.30 g, 79 % yield, Mp 37±1 °C) as a white solid. ^1H NMR (23 °C, 599.77 MHz, $CDCl_3$) δ ppm: 3.70 (s, 3H), 3.41 (t, 2H, $J_{1,2}$ = 12.0 Hz), 2.78 (t, 2H, $J_{1,2}$ = 12.0 Hz), 2.60 (t, 2H, $J_{1,2}$ = 12.0 Hz), 2.52 (t, 2H, $J_{1,2}$ = 12.0 Hz), 1.88-1.82 (m, 2H), 1.58-1.53 (m, 2H), 1.44-1.40 (m, 2H), 1.38-1.34 (m, 2H), 1.32-1.22 (brs, 16H),.^{13}C NMR (23 °C, 150.81 MHz, $CDCl_3$) δ ppm: 172.6 ($COOCH_3$), 51.9 (OCH_3),34.7, 34.1, 32.9, 32.2, 29.6-29.4 (CH_2x6), 29.3, 29.2, 28.9, 28.7, 28.1, 26.9, HRMS (ES) calcd for $C_{18}H_{35}O_2SBr(M^+)$ 394.15411, found 394.15227 and (M+2) at 396.0 (due to isotopic abundance).

Synthesis of 18-fluoro-4-thia-octadecanoic acid (9)—An anhydrous acetonitrile solution (3 mL) of bromo-ester **8** (80 mg, 0.20 mmol) and 1M THF solution of TBAF (3 mL, 3.0 mmol) were stirred at room temperature for 72 h under nitrogen (additional, 0.5 ml (0.5 mmol) 1M THF solution was further added at 24 h and 48 h). Solvent was evaporated under vacuum. The resulting solid was dissolved in 100 mL of dichloromethane, washed with water, dried over anhydrous Na_2SO_4 and filtered. The filtrate was evaporated under vacuum to dryness. The obtained fluoro-ester residue was further subjected to hydrolysis using 0.5 mL aqueous solution of KOH (10 mg, 0.18 mmol) and stirred at room temperature for 2 h. The solvent was evaporated under vacuum. The obtained residue was dissolved in 25 mL of dichloromethane, washed with 1N HCl, dried over Na_2SO_4 and filtered. The filtrate was evaporated under vacuum and purified by column chromatography using 4:96 methanol:chloroform as solvent and silica gel as an adsorbent to obtain compound **9** as a white solid (40 mg, 61.6 % overall yield, Mp 57±1 °C).^1H NMR (23 °C, 599.77 MHz, $CDCl_3$) δ ppm: 4.46 (dt, 2H, J_1 = 47.3 Hz, J_2 = 6.2 Hz), 2.82 (t, 2H, $J_{1,2}$ = 7.3 Hz), 2.70 (t, 2H, $J_{1,2}$ = 7.3 Hz), 2.57 (t, 2H, $J_{1,2}$ = 7.3 Hz), 1.74-1.68 (m, 2H), 1.63-1.58 (m, 2H), 1.42-1.38 (m, 4H), 1.32-1.22 (brs, 16H).^{13}C NMR (23 °C, 150.81 MHz, $CDCl_3$) δ ppm: 176.2, 84.8 and 83.7 (d, J = 163.8 Hz, F-CH_2 due to carbon-fluorine coupling), 34.3, 32.2, 30.4-30.3 (d, J= 19.6 Hz long range fluorine carbon coupling), 29.6-29.2 (CH_2x7), 29.2, 28.8, 26.6, 25.2, 25.1. HRMS (ES) calcd for $C_{17}H_{33}O_2SF(M^+)$ 320.21853, found 320.21755.

Synthesis of methyl 18-bromo-6-thia-octadecanoate (12)—Synthesis of methy18-fluoro-6-thia-octadecanoate (**12**) was achieved by coupling of methyl 6-mercaptopentanoate with 1, 12-dibromo dodecane (**11**) using sodium hydride. To a stirred solution of methyl 6-mercaptopentanoate (500 mg, 3.37 mmol) in anhydrous THF (100 mL) under nitrogen at 0

°C, NaH(81 mg, 3.37 mmol) was added. The resulting solution was stirred for additional 15 min at 0 °C. A solution of **11** (990 mg, 3.09 mmol) in THF (10 mL) was slowly added and the resulting mixture was maintained at 0 °C for 30 min. The mixture was then stirred for 3 h at room temperature and quenched with water. The dichloromethane extract was dried over Na_2SO_4, filtered and the filtrate was evaporated under vacuum. The residue was subjected to column chromatography (5:95 ethyl acetate:hexane) to yield compound **12** (1.09 g, 2.76 mmol, 82% yield) as a colorless oil. ^{1}H NMR (23 °C, 599.77 MHz, $CDCl_3$) δ ppm: 3.68 (s, 3H), 3.42 (t, 2H, $J_{1,2}$ = 12.0 Hz), 2.52-2.50 (m, 4H), 2.34 (t, 2H, $J_{1,2}$ = 12.0 Hz), 1.86-1.82 (m, 2H), 1.76-1.71 (m, 2H), 1.61-1.64 (m, 2H), 1.59-1.54 (m, 4H), 1.44-1.39 (m, 2H), 1.38-1.34 (m, 2H), 1.32-1.22 (brs, 10H).^{13}C NMR (23 °C, 150.81 MHz, $CDCl_3$) δ ppm: 174.1 ($COOCH_3$), 51.8 (OCH_3), 34.0, 33.6, 32.8, 32.1, 31.6, 29.6-28.7 (CH_2x9), 28.1, 24.1, HRMS (ES) calcd for $C_{18}H_{35}O_2SBr(M^+)$ 394.15411, found 394.15227 and (M+2) at 395.9 (due to isotopic abundance)

Synthesis of 18-fluoro-6-thia-octadecanoic acid (13)—An anhydrous acetonitrile solution (3 mL) of bromo-ester **12** (76 mg, 0.19 mmol) and 1M THF solution of TBAF (3 mL, 3.0 mmol) were stirred at room temperature for 72 h under nitrogen (additional, 0.5 ml (0.5 mmol) 1M THF solution was further added at 24 h and 48 h). Solvent was evaporated under vacuum. The resulting solid was dissolved in 100 mL of dichloromethane, washed with water, dried over anhydrous Na_2SO_4 and filtered. The filtrate was evaporated under vacuum to dryness. The obtained fluoro-ester residue was further subjected to hydrolysis using 0.5 mL aqueous solution of KOH (10 mg, 0.18 mmol) and stirred at room temperature for 2 h. The solvent was evaporated under vacuum. The obtained residue was dissolved in 25 mL of dichloromethane, washed with 1N HCl, dried over Na_2SO_4 and filtered. The filtrate was evaporated under vacuum and purified by column chromatography using 4:96 methanol:chloroform as solvent and silica gel as an adsorbent to obtain compound **13** as a white solid (38 mg, 61.7 % over all yield, Mp 51 ±1 °C).^{1}H NMR (23 °C, 599.77 MHz, $CDCl_3$)δ ppm: 4.46 (dt, 2H, J = 47.3 Hz, 6.2 Hz), 2.56-2.51 (m, 4H,), 2.41 (t, 2H, $J_{1,2}$ = 7.3 Hz), 1.79-1.66 (m, 6H), 1.61-1.58 (m, 2H), 1.40-1.38 (m, 4H), 1.33-1.29 (brs, 12H).^{13}C NMR (23 °C, 150.81 MHz, $CDCl_3$) δ ppm: 179.2, 84.8 and 83.7 (d, J = 163.5 Hz, **F-C**H_2 due to carbon-fluorine coupling), 33.7, 33.2, 32.1, 31.6, 30.4-30.3 (d, J= 19.1 Hz long range fluorine carbon coupling), 29.6-28.9 (CH_2x8), 25.1, 23.9. HRMS (ES) calcd for $C_{17}H_{33}O_2SF$ (M^+), 320.2151, found 320.2194.

General Procedure for ^{18}F-Labeling

The labeling precursors for all the four tracers **2**[3,6], **3**[10], **4**, and **5** were the methyl esters of their corresponding bromides (Schemes 1 and 2). Nucleophilic [^{18}F]fluorination and subsequent hydrolysis of the ester was performed as previously described[19]. Briefly, cyclotron-produced [^{18}F]fluoride was dried down under nitrogen at 95 °C in a 2 mL glass vial containing Kryptofix 2.2.2 (10 mg), acetonitrile (0.8 mL), and K_2CO_3 (4 mg) solution in water (0.15 mL). The residue was further dried by azeotropic distillation with acetonitrile (2 × 0.5 mL). A solution of the precursor (approximately 2–3 mg) in acetonitrile (0.5 mL) was added, and the vial was sealed (screw tight cap) and subjected to microwave irradiation at 75 °C for 5 min. Subsequent hydrolysis of the resulting [^{18}F]fluoro-ester was performed in the same vessel by the addition of 0.15 mL 0.2N KOH followed by microwave irradiation at 75 °C for 2 min. The mixture was then cooled, acidified with acetic acid (0.2 N), filtered, and injected on to the semi-preparative HPLC column (Phenomenex Luna C-18, 5μ, 10 × 250 mm). The mobile phase was acetonitrile/water/TFA (90:10:0.005 v/v) and flow rate was 5 mL/min (Rt = 9.4 min for **4** and Rt = 8.7 min for **5**). An in-line ultraviolet detector (210 nm) was used to monitor the elution of unlabeled materials. The [^{18}F]fluoro-fatty acid fraction was diluted in 50 mL water and trapped on a C-18 Sep-Pak cartridge (Accel C-18 Plus, Waters, Milford, MA), followed by washing of the Sep-Pak with 10 mL water. The

product was eluted from the Sep-Pak using 0.1 mL ethanol (multiple fractions). The fraction having highest activity was used for formulation in 0.5–1 % BSA in isotonic NaCl solution, and filtered through a 0.22 μ filter (Millex-GS, Millipore, Bedford, MA USA). Radiochemical purity (> 99 %) was analyzed by radio-HPLC in the system described above.

Biodistribution Studies in Rats

Female Sprague-Dawley rats were fasted overnight. The rats were anesthetized with isoflurane (3.5 % induction, 1.5 % maintenance). The ^{18}F-labeled radiotracer (0.7–1.4 MBq) was injected into the tail vein. The biodistributions were performed at either 30 min or 120 min before procurement of heart, liver, lung, blood, kidney, bone (femur), brain, and skeletal muscle. The tissues were counted for ^{18}F-radioactivity and weighed. All ^{18}F-radioactivity measurements were corrected for radioactivity decay. Radiotracer uptake was calculated as:

$$\text{Uptake}\,(\%\text{dose kg/g}) = \frac{\text{CPM (tissue)} \times \text{Body Wt.(kg)} \times 100}{\text{Tissue Wt.(g)} \times \text{CPM (dose)}} \quad \text{(Eq. 1)}$$

In one group of fasted rats, the CPT-I inhibitor POCA (30 mg/kg) was administered intraperitoneally 120 min prior to **3** injection. Crude analysis of the nature of the metabolites in the heart, liver and muscle was performed by a Folch-type extraction procedure. Approximately 0.5 g of tissue was excised and thoroughly homogenized and sonicated (20 s) in 7 mL chloroform/methanol (2:1) at 0 °C. Urea (40 %, 1.75 mL) and 5 % sulfuric acid (1.75 mL) were added and the mixture was sonicated for an additional 20 s. After centrifugation for 10 min at 1,800 g, aqueous, organic, and protein interphase (pellet) fractions were separated and counted for ^{18}F-radioactivity. Furthermore, the three fractions are obtained by this extraction method, an organic phase (chloroform/methanol), aqueous phase, and protein-pellet. The percentage of ^{18}F-radioactivity distributed among the three phases indicated the following: 1) organic phase contained non-metabolized fatty acid analog and complex lipid metabolites such as triglycerides and phospholipids; 2) aqueous phase contained F-18 fluoride or other aqueous soluble metabolites; and 3) the remaining protein-pellet contained protein-bound ^{18}F-labeled β-oxidation metabolites.

MicroPET/CT Imaging Studies in Rats

Female Sprague-Dawley rats were fasted overnight. The rats were anesthetized with isoflurane (3.5 % induction, 1.5 % maintenance). PET/CT scanning was performed using an eXplore Vista PET/CT (General Electric Health Care, Milwaukee, WI). The animal was positioned in the prone position with the snout positioned into the scanner. Before the radiotracer imaging study, a whole-body CT scan was performed. This scan was used for anatomical visualization and for attenuation correction of the emission data. The radiotracers were studied in different rats to allow the biodistribution to be done following the PET scan. The ^{18}F-labeled radiotracer (9–11 MBq) was injected into a tail vein, and the emission data were collected in dynamic acquisition for 50 min over the upper thorax, followed by a static whole-body scan from 55–115 min post-injection. For **3**–**5**, 2–5 rats were imaged with each tracer. In this preliminary study, representative images are presented for each ^{18}F-labeled fatty acid analog. The images were displayed as maximum intensity projections (MIPs) with coronal orientation. The pixel intensities were normalized to the highest pixel value within each image. The images were interpreted strictly qualitatively to show the imaging feasibility of the radiotracers as myocardial imaging agents and confirmation with the biodistribution data.

Statistical Analyses

All results were expressed as the mean ± SD. Comparison of the means was made using a two-tailed student's t-test. The acceptable level of significance was set at $p<0.05$. Microsoft Excel was used to perform the statistical analysis.

Supplementary Material

Refer to Web version on PubMed Central for supplementary material.

Acknowledgments

This work was supported by the National Institutes of Health (R01 HL-63371 (TRD), R01 CA108620 (TRD)), and the Department of Radiology, Brigham and Women's Hospital.

ABBREVIATIONS USED

FAO	fatty acid oxidation
CPT-I	carnitine palmitoyltransferase I
POCA	sodium 2-[5-(4-chlorophenyl)-pentyl]-oxirane-2-carboxylate
PET	positron emission tomography
CD36	cluster of differentiation 36 is an integral membrane protein
FATP	fatty-acid transport protein
CAT	carnitine acyl-carnitine translocase
1,14(R,S)	[^{18}F]fluoro-6-thia-heptadecanoic acid
(16:0)	sixteen carbon chain with no double bond
(18:0)	eighteen carbon chain with no double bond
(18:1)	eighteen carbon chain with one double bond
LAH	lithium aluminum hydride
THF	tetrahydrofuran
BSA	bovine serum albumin
TBAF	tetrabutyl ammonium fluoride
p.i	post-injection
amu	atomic mass unit

References

1. Lopaschuk GD, Ussher JR, Folmes CDL, Jaswal JS, Stanley WC. Myocardial fatty acid metabolism in health and disease. Physiol Rev. 2010; 90:207–258. [PubMed: 20086077]
2. DeGrado TR, Coenen HH, Stocklin G. 14(R,S)-[^{18}F]fluoro-6-thia-heptadecanoic acid (FTHA): evaluation in mouse of a new probe of myocardial utilization of long chain fatty acids. J Nucl Med. 1991; 32:1888–1896. [PubMed: 1919727]
3. DeGrado TR, Wang S, Holden JE, Nickles RJ, Taylor M, Stone CK. Synthesis and preliminary evaluation of ^{18}F-labeled 4-thia palmitate as a PET tracer of myocardial fatty acid oxidation. Nucl Med Biol. 2000; 27:221–231. [PubMed: 10832078]
4. Bergmann SR, Weinheimer CJ, Markham J, Herrero P. Quantitation of myocardial fatty acid metabolism using PET. J Nucl Med. 1996; 37:1723–1730. [PubMed: 8862319]

5. Pandey MK, Bansal A, DeGrado TR. Fluorine-18 labeled thia fatty acids for PET imaging of fatty acid oxidation in heart and cancer. Heart Metab. 2011; 51:15–19.
6. DeGrado TR, Kitapci MT, Wang S, Ying J, Lopaschuk GD. Validation of ^{18}F-fluoro-4-thia-palmitate as a PET probe for myocardial fatty acid oxidation: effects of hypoxia and composition of exogenous fatty acids. J Nucl Med. 2006; 47:173–181. [PubMed: 16391202]
7. Wallhaus TR, Taylor M, DeGrado TR, Russell DC, Stanko P, Nickles RJ, Stone CK. Myocardial free fatty acid and glucose use after carvedilol treatment in patients with congestive heart failure. Circulation. 2001; 103:2441–2446. [PubMed: 11369683]
8. Renstrom B, Rommelfanger S, Stone CK, DeGrado TR, Carlson KJ, Scarbrough E, Nickles RJ, Liedtke AJ, Holden JE. Comparison of fatty acid tracers FTHA and BMIPP during myocardial ischemia and hypoxia. J Nucl Med. 1998; 39:1684–1689. [PubMed: 9776269]
9. Stone CK, Pooley RA, DeGrado TR, Renstrom B, Nickles RJ, Nellis SH, Liedtke AJ, Holden JE. Myocardial uptake of the fatty acid analog 14-fluorine-18-fluoro-6-thia-heptadecanoic acid in comparison to beta-oxidation rates by tritiated palmitate. J Nucl Med. 1998; 39:1690–1696. [PubMed: 9776270]
10. DeGrado TR, Bhattacharyya F, Pandey MK, Belanger AP, Wang S. Synthesis and preliminary evaluation of 18-[^{18}F] fluoro-4-thia-oleic acid (FTO) as a PET probe of fatty acid oxidation. J Nucl Med. 2010; 51:1310–1317. [PubMed: 20660391]
11. Jain SC, Kumar R, Goswami R, Pandey MK, Khurana S, Rohatgi L, Gyanda K. Synthesis of novel non-isoprenoid phenolic acids and 3-alkylpyridines. Pure Appl Chem. 2005; 177:185–193.
12. Belanger AP, Pandey MK, DeGrado TR. Microwave-assisted radiosynthesis of [^{18}F] fluorinated fatty acid analogs. Nucl Med Biol. 2011; 38:435–441. [PubMed: 21492792]
13. Jung CM, Kraus W, Leibnitz P, Pietzsch HJ, Kropp J, Spies H. Synthesis and first crystal structure of rhenium complexes derived from ω-functionalized fatty acids as model compounds of technetium tracers for myocardium metabolism imaging. Eur J Inorg Chem. 2002:1219–1225.
14. DeGrado TR, Holden JE, Ng CK, Raffel DM, Gatley SJ. Comparision of 16-iodohexadecanoic acid (IHDA) and 15-p-iodophenlpentadecanoic acid (IPPA) metabolism and kinetics in the isolated rat heart. Eur J Nucl Med. 1988; 14:600–606. [PubMed: 3243308]
15. Ouellet V, Labbé SM, Blondin DP, Phoenix S, Brigitte Guérin B, Haman F, Turcotte EE, Richard D, Carpentier AC. Brown adipose tissue oxidative metabolism contributes to energy expenditure during acute cold exposure in humans. J Clin Invest. 2012; 122(2):545–552. [PubMed: 22269323]
16. Folmes CD, Clanachan AS, Lopaschuk GD. Fatty acid oxidation inhibitors in the management of chronic complications of atherosclerosis. Curr Atheroscler Rep. 2005; 7:63–70. [PubMed: 15683605]
17. Di Napoli P, Taccardi AA, Barsotti A. Long term cardioprotective action of trimetazidine and potential effect on the inflammatory process in patients with ischaemic dilated cardiomyopathy. Heart. 2005; 91:161–165. [PubMed: 15657223]
18. Wambolt RB, Lopaschuk GD, Brownsey RW, Allard MF. Dichloroacetate improves postischemic function of hypertrophied rat hearts. J Am Coll Cardiol. 2000; 36:1378–1385. [PubMed: 11028498]
19. Knust EJ, Kupfernagel C, Stocklin G. Long-chain F-18 fatty acids for the study of regional metabolism in heart and liver; odd-even effects of metabolism in mice. J Nucl Med. 1979; 20:1170–1175. [PubMed: 317095]
20. Fox KA, Abendschein DR, Ambos HD, Sobel BE, Bergmann SR. Efflux of metabolized and nonmetabolized fatty acid from canine myocardium. Implications for quantifying myocardial metabolism tomographically. Circ Res. 1985; 57:232–243. [PubMed: 4017196]
21. Livni E, Elmaleh DR, Barlai-Kovach MM, Goodman MM, Knapp FF Jr, Strauss HW. Radioiodinated beta-methyl phenyl fatty acids as potential tracers for myocardial imaging and metabolism. Eur Heart J. 1985; 6(Suppl, B):85–89. [PubMed: 4085510]
22. Livni E, Elmaleh DR, Levy S, Brownell GL, Strauss WH. Beta-methyl[1-^{11}C]heptadecanoic acid: a new myocardial metabolic tracer for positron emission tomography. J Nucl Med. 1982; 23:169–175. [PubMed: 6977020]

23. DeGrado TR, Holden JE, Ng CK, Raffel DM, Gatley SJ. β-Methyl-15-p-iodophenylpentadecanoic acid metabolism and kinetics in the isolated rat heart. Eur J Nucl Med. 1989; 15:78–80. [PubMed: 2920741]

24. Goodman MM, Knapp FF Jr, Callahan AP, Ferren LA. Synthesis and biological evaluation of 17-[^{131}I]iodo-9-telluraheptadecanoic acid, a potential imaging agent. J Med Chem. 1982; 25:613–618. [PubMed: 7097713]

25. Moka DC, DeGrado TR. Non-β-oxidizable ω-[^{18}F]fluoro long chain fatty acid analogs show cytochrome P-450-mediated defluorination: Implications for the design of PET tracers of myocardial fatty acid utilization. International Journal of Radiation Applications and Instrumentation. Part B Nuclear Medicine and Biology. 1992; 19:389–397.

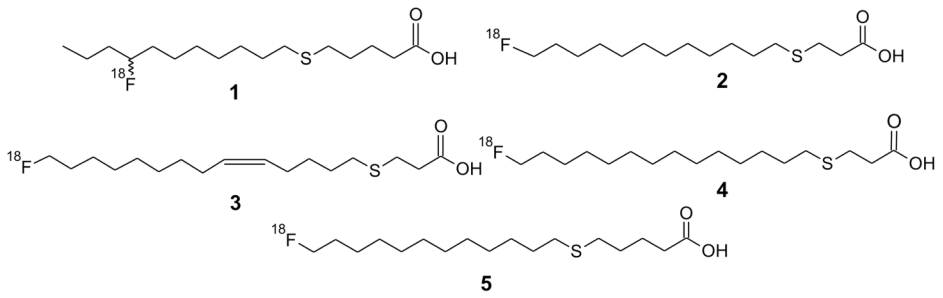

Figure 1.
Structure of thia-substituted fatty acids synthesized and evaluated as metabolically trapped myocardial FAO probes.

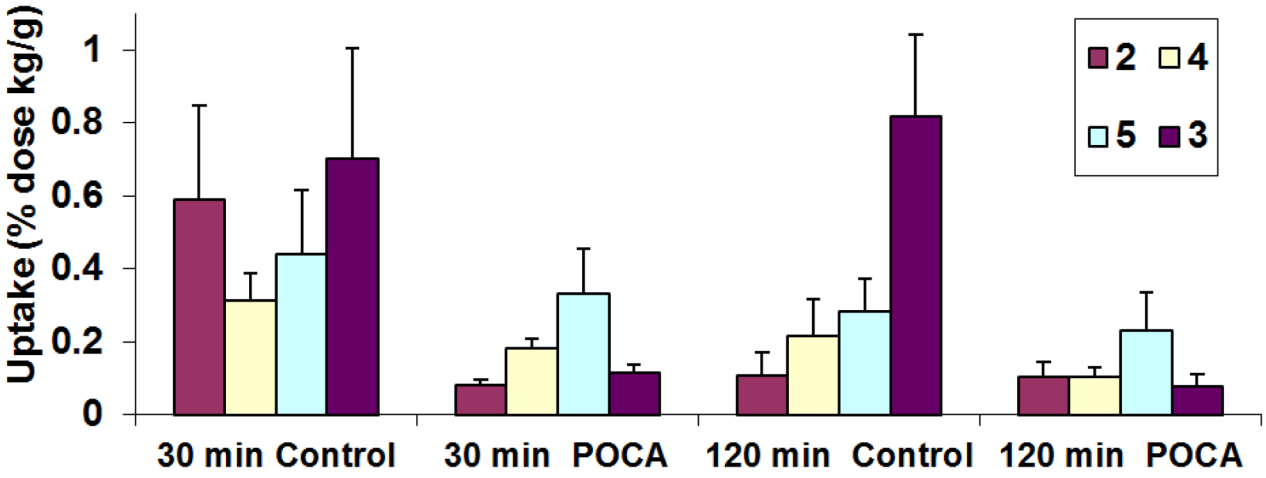

Figure 2.

Comparison of heart uptake of **2–5** in fasted rats. Compound **3** uptake at 120 m in control rats is statistically higher than for **2**, **4**, and **5** (p= <0.05). Compound **3** showed the highest degree of blockade of heart uptake at both 30 m and 120 m time points. (The data are derived from Tables 2–4)

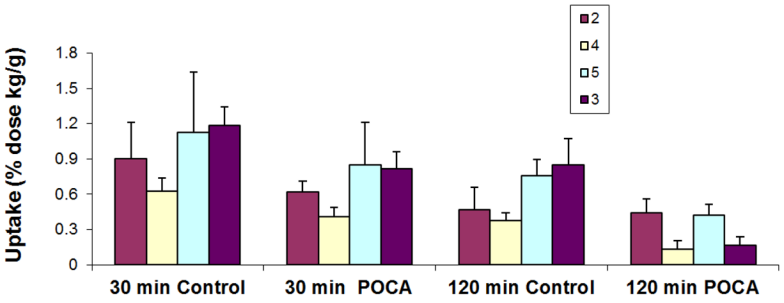

Figure 3.

Comparison of liver uptake of **2–5** in fasted rats. Compounds **3** and **4** showed the highest degree of blockade of liver uptake at 120 m time point (p=<0.05). (The data are derived from Tables 2–4)

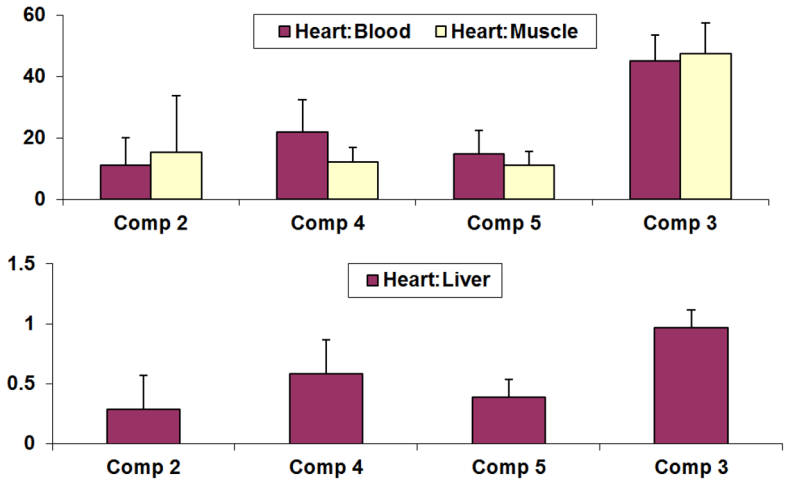

Figure 4.

Comparison of heart:blood, heart:muscle and heart:liver ratios for compounds **2–5** in fasted rats at 120 min p.i. (heart:blood, and heart:muscle are statistically higher for **3** than for **2**, **4**, and **5** ($p = <0.05$), for heart:liver values for **3** are also statistically higher than for **2** and **5** ($p = <0.05$). (The data are derived from Tables 2–4)

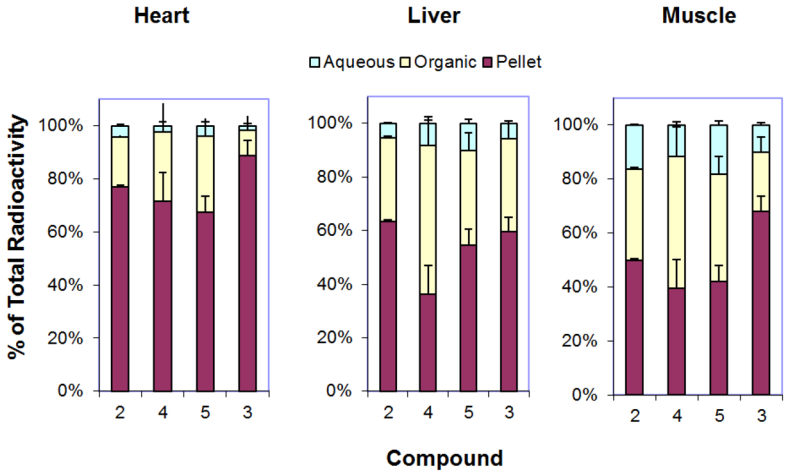

Figure 5.
Folch-type extraction analysis of metabolites at 120 min (p.i) in control Sprague-Dawley rats. (The data are derived from Table 5)

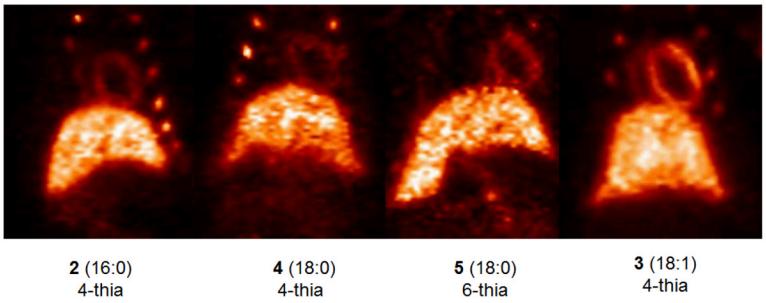

Figure 6.

Representative MicroPET Images of **2–5** at 55–115 min p.i. Images are presented as maximum intensity projections (MIPs) of rats in coronal orientation with snout up. Accumulation of the radiotracers is visualized in heart, liver and ribs (evidencing defluorination).

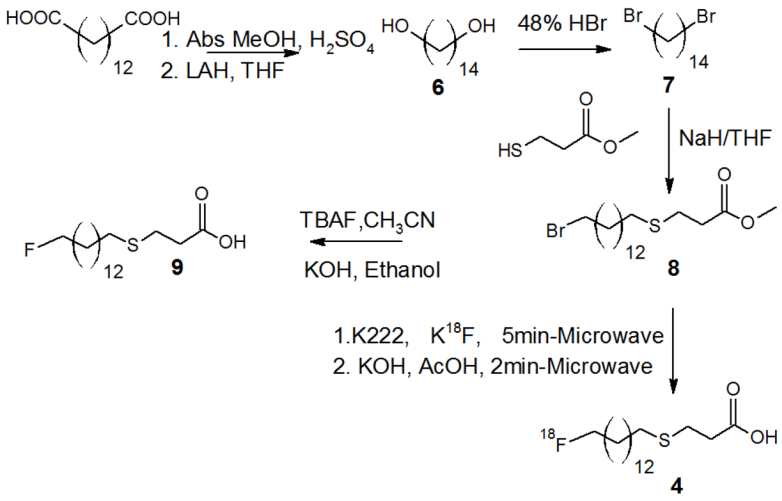

Scheme 1.
Synthesis of 18-[^{18}F]fluoro-4-thia-octadecanoic acid (**4**)

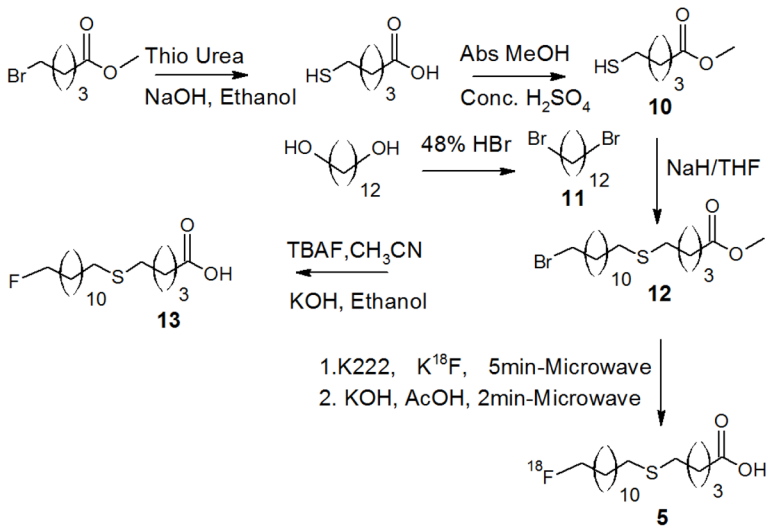

Scheme 2.
Synthesis of 18-[^{18}F]fluoro-6-thia-octadecanoic acid (**5**)

Table 1

Uptake (% dose kg/g) of 16-[^{18}F]fluoro-4-thia-hexadecanoic acid (**2**) in fasted Sprague-Dawley rats

ORGAN/TISSUE (N = 6)	CONTROL 30 MIN¶	POCA TREATED 30 MIN*	CONTROL 120 MIN¶	POCA TREATED 120 MIN*
Blood	0.070±0.059	0.0633±0.0077	0.0105±0.0028	0.0392±0.0094#
Heart	0.589±0.257£	0.0792±0.0174€	0.1069±0.0649	0.1042±0.0387
Lung	0.099±0.140	0.0676±0.0126	0.0183±0.0072	0.0472±0.0098#
Liver	0.899±0.314	0.6197±0.0949	0.4700±0.1888	0.4433±0.1201
Kidney	0.209±0.144	0.2477±0.0310	0.1014±0.0512	0.1637±0.0659
Brain	0.067±0.049£	0.04879±0.0142	0.0154±0.0056	0.0578±0.0114#
Bone	0.235±0.168	0.1790±0.0758	0.3143±0.1334	0.6549±0.1112#
Muscle	0.031±0.013£	0.0333±0.0080	0.0109±0.0059	0.0298±0.0069#

*Pretreated with POCA (30 mg/kg i.p.) 2 hr prior

¶data from ref. 10

#p<0.05 for 120 m control vs 120 m POCA

£p<0.05 for 30 m control vs 120 m control

€p<0.01 for 30 m control vs 30 m POCA

Table 2

Uptake (% dose kg/g) of 18-[^{18}F]fluoro-4-thia-octadecanoic acid (**4**) in fasted Sprague-Dawley rats

ORGAN/TISSUE (N = 6)	CONTROL 30 MIN	POCA TREATED 30 MIN*	CONTROL 120 MIN	POCA TREATED 120 MIN*
Blood	0.0392±0.0063	0.0510±0.0026£	0.0098±0.0006**	0.0125±0.0033
Heart	0.3140±0.0738	0.1814±0.0276£	0.2144±0.1017**	0.1025±0.0260
Lung	0.0755±0.0168	0.0998±0.0245	0.0339±0.0122**	0.0244±0.0092
Liver	0.6292±0.1114	0.4064±0.0787£	0.3759±0.0655**	0.1341±0.0686€
Kidney	0.1872±0.0248	0.2350±0.0199£	0.0726±0.0166**	0.0947±0.0350
Brain	0.0200±0.0037	0.0385±0.0033£	0.0143±0.0015	0.0310±0.0111€
Bone	0.2309±0.0588	0.2289±0.0332	0.2934±0.0826	0.4042±0.0612€
Muscle	0.0303±0.0061	0.0443±0.0047£	0.0181±0.0070**	0.0197±0.0060

*Pretreated with POCA (30 mg/kg i.p.) 2 hr prior

£p<0.05 for 30 m control vs 30 m POCA

**p<0.05 for 30 m control vs 120 m control

€p<0.05 for 120 m control vs 120 m POCA

Table 3

Uptake (% dose kg/g) of 18-[^{18}F]fluoro-6-thia-octadecanoic acid (**5**) in fasted Sprague-Dawley rats

ORGAN/TISSUE (N = 6)	CONTROL 30 MIN	POCA TREATED 30 MIN*	CONTROL 120 MIN	POCA TREATED 120 MIN*
Blood	0.0290±0.0120	0.0510±0.0190£	0.0241±0.0137	0.0271±0.0038
Heart	0.4413±0.1749	0.3331±0.1210	0.2815±0.0895	0.2288±0.1051
Lung	0.0621±0.0180	0.1163±0.0421	0.0702±0.0118	0.0536±0.0090
Liver	1.1260±0.5112	0.8492±0.3636	0.7548±0.1403	0.4190±0.0941€
Kidney	0.2095±0.0734	0.3441±0.1484	0.1629±0.0587	0.1554±0.0249
Brain	0.0330±0.0223	0.0879±0.0479	0.0220±0.0041	0.0519±0.0124€
Bone	0.1171±0.0493	0.1037±0.0297	0.2467±0.0766**	0.2104±0.0494
Muscle	0.0390±0.0268	0.0639±0.0242	0.0263±0.0063	0.0599±0.0127

*Pretreated with POCA (30 mg/kg i.p.) 2 hr prior

£p<0.05 for 30 m control vs 30 m POCA

**p<0.05 for 30 m control vs 120 m control

€p<0.05 for 120 m control vs 120 m POCA

Table 4

Uptake (% dose kg/g) of 18-[^{18}F]fluoro-4-thia-(9*Z*)-octadec-9-enoic acid (**3**) in fasted Sprague-Dawley rats

ORGAN/TISSUE (N = 5)	CONTROL 30 MIN*¶	POCA TREATED 30 MIN	CONTROL 120 MIN	POCA TREATED 120 MIN*¶
Blood	0.0441±0.0121	0.0606±0.0096	0.0185±0.005**	0.0141±0.0098
Heart	0.7028±0.3019	0.1155±0.0211£	0.8164±0.2249	0.0760±0.0360
Lung	0.0496±0.0096	0.0458±0.0061	0.0228±0.005**	0.0179±0.0109
Liver	1.1847±0.1550	0.8162±0.1420£	0.8488±0.2232**	0.1666±0.0706€
Kidney	0.2035±0.0510	0.1932±0.0173	0.1244±0.0310	0.0611±0.0222€
Brain	0.0206±0.0057	0.0368±0.0044£	0.0215±0.0051	0.0206±0.009
Bone	0.1531±0.0796	0.1475±0.0355	0.4610±0.4140	0.2990±0.1645
Muscle	0.0201±0.007	0.0297±0.0039£	0.0171±0.0024	0.0216±0.0137

*Pretreated with POCA (30 mg/kg i.p.) 2 hr prior

¶ref 10

£p=<0.05 for 30 m control vs 30 m POCA

**p=<0.05 for 30 m control vs 120 m control

€p=<0.05 for 120 m control vs 120 m POCA

J Med Chem. Author manuscript; available in PMC 2012 December 31.

Table 5

Distribution of ^{18}F-radioactivity (% of total) in aqueous, organic and pellet fractions after Folch-Type extraction of tissues

Compound		30 min Control	30 min POCA[a]	120 min Control	120 min POCA[a]
2					
Heart (n =6)	Aqueous	2.63±1.00	15.28±3.96[b]	4.17±1.31	7.53±2.25[b]
	Organic	38.56±19.03	51.90±3.86	18.88±10.79	67.98±6.82[b]
	Pellet	58.80±19.21	32.81±6.12[b]	76.93±10.77	24.47±5.35[b]
Liver (n =6)	Aqueous	13.52±8.30	20.23±4.88	5.32±0.82	11.52±1.13[b]
	Organic	48.25±8.35	41.68±6.53	31.39±9.80	50.00±8.31[b]
	Pellet	38.21±13.23	38.07±4.09	63.27±9.25	38.47±8.58[b]
Muscle (n =6)	Aqueous	23.24±8.37	25.13±2.90	16.17±4.64	19.16±4.09
	Organic	33.56±13.11	42.23±6.23	34.00±12.3	48.14±7.73
	Pellet	43.18±16.90	32.63±5.99	49.81±16.94	32.69±5.13
3					
Heart (n =5)	Aqueous	2.86±1.55	10.15±2.55[b]	1.86±0.37	4.19±1.04[b]
	Organic	8.46±0.86	62.03±7.43[b]	9.34±0.42	66.66±11.65[b]
	Pellet	88.67±1.63	23.80±5.76[b]	88.78±0.71	29.14±10.80[b]
Liver (n =5)	Aqueous	8.43±1.10	16.30±3.66[b]	5.68±0.19	8.10±2.07
	Organic	19.87±3.32	58.80±4.90[b]	34.75±12.14	68.06±3.39[b]
	Pellet	71.69±4.34	24.88±3.54[b]	59.56±12.02	23.82±3.75[b]
Muscle (n=5)	Aqueous	18.79±3.83	24.06±5.81	9.91±2.52	11.37±1.57
	Organic	21.75±4.86	43.19±4.95[b]	21.98±4.18	53.25±9.73[b]
	Pellet	59.12±8.66	32.74±6.02[b]	67.95±1.75	35.36±11.08[b]
4					
Heart (n =6)	Aqueous	3.97±1.01	7.73±0.62[b]	2.39±0.95	3.39±3.17
	Organic	17.29±2.61	67.58±3.94[b]	26.14±5.50	74.91±6.52[b]
	Pellet	78.72±3.49	24.67±3.92[b]	71.45±5.49	21.68±3.63[b]

Compound		30 min Control	30 min POCA[a]	120 min Control	120 min POCA[a]
Liver (n =6)	Aqueous	15.36±1.68	31.69±5.95[b]	8.18±4.73	10.23±3.80
	Organic	51.66±5.80	51.76±7.03	55.69±8.48	67.69±13.75
	Pellet	32.97±6.71	16.53±1.87[b]	36.13±11.75	22.07±13.63
Muscle (n =6)	Aqueous	28.99±3.73	25.80±5.01	11.58±3.65	9.12±2.18
	Organic	38.77±5.36	47.15±2.67[b]	48.90±7.54	58.25±8.75
	Pellet	32.22±5.24	27.04±3.35	39.51±4.831	32.62±8.20
5					
Heart (n =6)	Aqueous	4.02±1.24	3.84±1.31	4.03±1.42	3.30±1.07
	Organic	25.81±10.12	63.99±9.67[b]	28.56±6.62	74.20±7.78[b]
	Pellet	70.16±9.05	32.16±10.47[b]	67.39±6.01	22.48±6.91[b]
Liver (n =6)	Aqueous	9.65±3.27	10.75±2.01	10.15±4.50	7.45±2.00
	Organic	45.61±5.10	54.88±6.96	35.26±4.02	64.78±10.98[b]
	Pellet	44.72±4.54	34.35±7.76	54.58±5.08	27.76±9.07[b]
Muscle (n =6)	Aqueous	16.49±2.26	7.70±2.81[b]	18.18±5.46	9.30±1.56[b]
	Organic	44.55±8.06	43.43±11.19	39.74±10.78	59.27±6.95[b]
	Pellet	38.95±7.41	48.85±12.63	42.06±9.84	31.41±7.23

[a]Pretreated with POCA (30 mg/kg i.p.) 2 hr prior.

[b]p=<0.05 for control vs POCA

Table 6

Plasma concentration of metabolic substrates in Sprague-Dawley rats

	Fatty Acid (mM)	Glucose (mg/dl)	Triglyceride (mg/dl)	Lactate (mmol)
Control (n=12)	0.242±0.161	111.660 ±14.768	46.484±36.701	1.797±0.577
POCA (n= 6)	0.905±0.085	66.748±15.945	47.971±18.730	1.850±0.523
P value	4.84E-09	0.000226	0.9107	0.8470